

42. E. T. Walters and J. H. Byrne, *Brain Res.* **280**, 165 (1983).
43. We thank M. Barish, M. Fanselow, F. Krasne, and T. O'Dell for their helpful comments on the manuscript. Supported by grants from the National Institutes of Health (NS29563), the National Science Foundation (IBN-9410579), the Alzheimer's Disease Program,

State of California Department of Health Services (95-23335), and the Academic Senate, University of California, Los Angeles, to D.L.G. as well as by a grant from the National Institute of Mental Health (F31-MH11136) to G.G.M.

13 May 1997; accepted 18 August 1997

Inhibition of Phosphatases and Increased Ca^{2+} Channel Activity by Inositol Hexakisphosphate

Olof Larsson, Christopher J. Barker, Åke Sjöholm, Håkan Carlqvist, Robert H. Michell, Alejandro Bertorello, Thomas Nilsson, Richard E. Honkanen, Georg W. Mayr, Jean Zwiller, Per-Olof Berggren*

Inositol hexakisphosphate (InsP_6), the dominant inositol phosphate in insulin-secreting pancreatic β cells, inhibited the serine-threonine protein phosphatases type 1, type 2A, and type 3 in a concentration-dependent manner. The activity of voltage-gated L-type calcium channels is increased in cells treated with inhibitors of serine-threonine protein phosphatases. Thus, the increased calcium channel activity obtained in the presence of InsP_6 might result from the inhibition of phosphatase activity. Glucose elicited a transient increase in InsP_6 concentration, which indicates that this inositol polyphosphate may modulate calcium influx over the plasma membrane and serve as a signal in the pancreatic β cell stimulus-secretion coupling.

Depolarization-induced opening of voltage-gated L-type Ca^{2+} channels results in an increase in cytoplasmic free Ca^{2+} concentration ($[\text{Ca}^{2+}]_i$) and is one of the main features of the stimulus-secretion coupling in insulin-secreting cells (1). Under physiological conditions, depolarization is initiated by rapid uptake and phosphorylation of glucose, which result in the closure of adenosine triphosphate (ATP)-regulated K^+ channels. Insulin-secreting cells also have a number of receptors whose activation regulates the intracellular concentration of inositol polyphosphates (2). Although a large number of inositol polyphosphates have been identified in eukaryotic cells (3), except for the inositol 1,4,5-trisphosphate-induced mobilization of Ca^{2+} from intracellular stores, little is known about their roles in cell regulation. Protein phosphorylation

modulates the activity of voltage-sensitive ion channels (4), and in insulin-secreting cells, the activity of voltage-gated L-type Ca^{2+} channels is increased by inhibition of serine-threonine protein phosphatases (PPases) (5, 6).

We examined the inositol phosphates present in insulin-secreting cells after labeling them for 168 hours with $[2\text{-}^3\text{H}]\text{myo}$ -inositol (Fig. 1), when all inositol phosphates are at isotopic equilibrium (7, 8). InsP_6 was the dominant inositol phosphate in hamster insulin-secreting (HIT) cells, as it is in other mammalian cells (9). An inositol-containing compound that is more polar than InsP_6 , most likely a pyrophosphate derivative (9), was also present. Enzyme assays and immunoblots of cell ho-

mogenates showed that the cells contained serine-threonine PPases that were inhibited by okadaic acid (OA), microcystin-LR, calyculin-A, and nodularin (10). Inhibition of the serine-threonine PPases type 1 (PP1), type 2 (PP2A), and type 3 (PP3) in insulin-secreting cells, which may enhance phosphorylation of the voltage-gated L-type Ca^{2+} channel or an associated protein, results in an increase in channel open probability, $[\text{Ca}^{2+}]_i$, and insulin release (5, 6).

InsP_6 , at concentrations similar to those present in insulin-secreting cells (40 to 54 μM) (11), suppressed the activities of PP1, PP2A, and PP3 in a concentration-dependent manner, with inhibition constant K_i values at or below $\sim 10 \mu\text{M}$ (Fig. 2A and Table 1) (12). The inhibitory effects of InsP_6 on PPase activities were similar to those of OA (13). Two isomers of inositol pentakisphosphate (InsP_5), $\text{Ins}(1,3,4,5,6)\text{P}_5$ and $\text{Ins}(1,2,3,4,6)\text{P}_5$, were one-half to one-fifth as potent, depending on the particular combination of InsP_5 and PPase (Fig. 2, C and D). $\text{Ins}(1,2,3,4,6)\text{P}_5$, like InsP_6 , includes a 1,2,3-trisphosphate array that binds Fe^{3+} and probably other cations (14). However, the fact that $\text{Ins}(1,2,3,4,6)\text{P}_5$ has a lower potency than InsP_6 indicates that this type of chelation is not the primary mechanism in PPase inhibition (15). Whereas PP3 was the most selective for InsP_6 , PP1 was the least selective, and PP2A fell in between (Table 1). However, neither the dominant inositol tetraphosphate (InsP_4) in these cells, $\text{Ins}(3,4,5,6)\text{P}_4$, nor the other major InsP_4 , $\text{Ins}(1,3,4,5)\text{P}_4$, had any inhibitory effect up to 100 μM (16). The fact that removal of one or two of the six phosphate groups from InsP_6 either reduced or abolished these effects indicates that PPase inhibition by InsP_6 is specific and is not simply an effect of a concentrated array of monoester phosphate groups. Inositol hexasulfate (InsS_6), which presents a charge array similar to that of InsP_6 , was about one-fourteenth as potent an inhibitor of PP2A and PP3 (Fig. 2B and Table 1). InsP_6 is

Table 1. K_i values of various inositol polyphosphates for the inhibition of the three serine-threonine PPases. The values for K_i and SEM were obtained by analysis of the data by nonlinear regression, fitting the data to sigmoidal dose-response curves generated by software (Prism; GraphPAD, San Diego, California). Values were obtained by one-way ANOVA with P values corrected for multiple comparisons by the Bonferroni method (Instat). Significant differences between the K_i values of InsP_6 and other inositol derivatives for each PPase are shown (* $P < 0.05$, ** $P < 0.01$, and *** $P < 0.001$). ND, not determined.

Inositol derivative	$K_i(\mu\text{M}) \pm \text{SEM}$		
	PPase 1 ($n = 4$)	PPase 2A ($n = 6$)	PPase 3 ($n = 6$)
InsP_6	13.40 ± 1.27	8.54 ± 1.11	3.85 ± 1.02
$\text{Ins}(1,3,4,5,6)\text{P}_5$	$6.47 \pm 1.50^*$	12.69 ± 1.28	$13.5 \pm 1.18^{**}$
$\text{Ins}(1,2,3,4,6)\text{P}_5$	ND	$40.5 \pm 1.10^{***}$	$21.5 \pm 1.76^{***}$
InsS_6	$29.9 \pm 1.87^{***}$	$116 \pm 1.02^{***}$	$55.0 \pm 1.25^{***}$

O. Larsson, C. J. Barker, Å. Sjöholm, A. Bertorello, T. Nilsson, P.-O. Berggren, Rolf Luft Center for Diabetes Research, Department of Molecular Medicine, Karolinska Institute, S-171 76 Stockholm, Sweden.

H. Carlqvist, Astra Pain Control AB, Cellular and Molecular Pharmacology, Novum Unit, S-141 57 Huddinge, Sweden.

R. H. Michell, School of Biochemistry, University of Birmingham, Post Office Box 363, Birmingham B15 2TT, UK.

R. E. Honkanen, Department of Biochemistry, MSB 2198, College of Medicine, University of South Alabama, Mobile, AL 36688, USA.

G. W. Mayr, Institut für Physiologische Chemie, Universitäts-Krankenhaus Eppendorf, 20246 Hamburg, Germany. J. Zwiller, INSERM U338, 5 rue B. Pascal, 67084 Strasbourg, France.

*To whom correspondence should be addressed.

more abundant than any of the InsP_5 isomers in β cells and is thus the only inositol polyphosphate that is likely to affect the activities of the PPases in vivo. InsP_6 also inhibited PPase activity in a cell homogenate, although slightly less potently ($K_i \sim 20 \mu\text{M}$) (Fig. 2E). This inhibition indicates that the inhibitory effect of InsP_6 on the catalytic subunits is maintained on serine-threonine phosphatase complexes present in insulin-secreting cells. The lower potency may reflect the presence in the cell homogenates of multiple proteins that bind InsP_6 (17–20).

We measured the effects of InsP_6 on whole cell Ca^{2+} currents in insulin-secreting cells (Fig. 3) (21). The cells were depolarized to 0 mV, from a holding potential of -80 mV, every 20 s. The Ca^{2+} current (I_{Ca}) increased severalfold when $10 \mu\text{M}$ InsP_6 was included in the pipette solution (Fig. 3A). The stimulatory effect of InsP_6 on Ca^{2+} channel activity varied between passages as well as between various batches of cells, perhaps reflecting cellular variability in basal PPase activity. Typically, in a batch of responding cells, I_{Ca} increased in about 30% of the cells, with the InsP_6 -induced increase observed at the second or third depolarizing pulse (that is, after 40 to 60 s) after establishment of the whole cell configuration. In traces, averaged from 30 of the responding cells, InsP_6 both increased peak current and reduced the rate of inactivation of the I_{Ca} (Fig. 3B). The effect of InsP_6 on peak I_{Ca} was about three times as pronounced as that previously evoked by OA, when similar cells and experimental protocol were applied (5). Inclusion of InsP_6 in the pipette did not change the pattern of the current-voltage relation (Fig. 4A).

Insulin-secreting cells contain various types of voltage-gated Ca^{2+} channels, but the L and T types are dominant (22). The

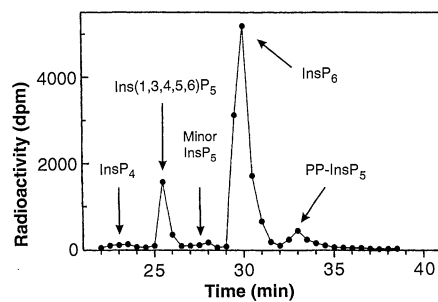


Fig. 1. Profile of inositol phosphates present in insulin-secreting cells. Cells were labeled for 168 hours with $[2\text{-}^3\text{H}]\text{myo-inositol}$ ($2 \mu\text{Ci/ml}$), resulting in isotopic equilibrium for all inositol phosphates (7), and inositol phosphates were extracted and separated by HPLC (8). The profile shown is representative of three experiments that were performed.

current induced by exposure of cells to InsP_6 was typical of the L-type Ca^{2+} channel, with slow inactivation properties. Because $20 \mu\text{M}$ Cd^{2+} blocks only L-type Ca^{2+} channels (23) and abolished the stimulatory effect of InsP_6 on whole cell Ca^{2+} currents (Fig. 3Dii), the T-type Ca^{2+} channel appears not to be involved. The stimulatory effect was maintained for at least 10 min in the presence of InsP_6

(24). The effect of $\text{Ins}(1,3,4,5,6)\text{P}_5$ and $\text{Ins}(1,2,3,4,6)\text{P}_5$ on Ca^{2+} channel activity reflected the K_i values of these inositol polyphosphates on PPase activity, in that a higher concentration of InsP_5 ($50 \mu\text{M}$) than of InsP_6 was needed to promote Ca^{2+} channel activity (Fig. 4, B and C). The InsP_5 isomers did not alter the rate of inactivation of the Ca^{2+} channels, and there was no difference in effects of the

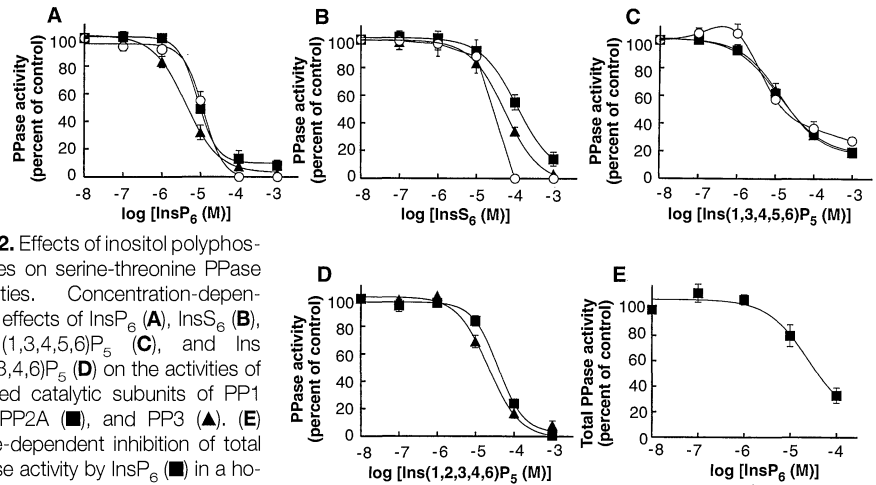
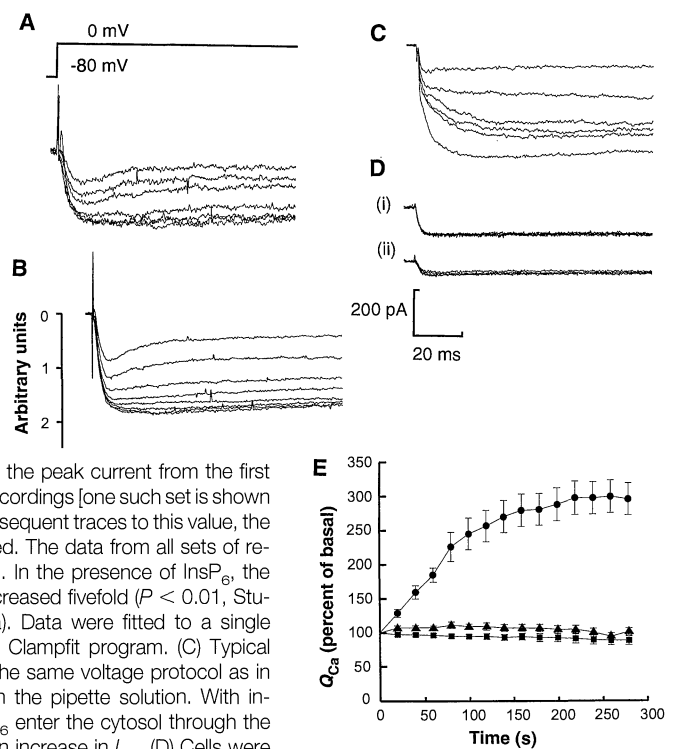


Fig. 2. Effects of inositol polyphosphates on serine-threonine PPase activities. Concentration-dependent effects of InsP_6 (A), InsS_6 (B), $\text{Ins}(1,3,4,5,6)\text{P}_5$ (C), and $\text{Ins}(1,2,3,4,6)\text{P}_5$ (D) on the activities of purified catalytic subunits of PP1 (○), PP2A (■), and PP3 (▲). (E) Dose-dependent inhibition of total PPase activity by InsP_6 (■) in a homogenate of insulin-secreting cells. Each point is the mean \pm SEM of duplicate values, expressed as the phosphatase activity with no added inositol phosphate, of four (for PP1), six (for PP2A and PP3), and three (total PPase) separate experiments.

Fig. 3. Effects of InsP_6 and InsS_6 on I_{Ca} in insulin-secreting cells. Whole cell Ca^{2+} channel currents were evoked by repetitive depolarizing voltage steps (100 ms) every 20 s to a membrane potential of 0 mV from a holding potential of -80 mV (A to E). (A) Sample traces showing inward current I_{Ca} generated by the actual depolarizing protocol and with $10 \mu\text{M}$ InsP_6 in the pipette solution. (B) Compiled data on inward I_{Ca} from 30 responding cells in the presence of InsP_6 . By setting the peak current from the first depolarization in each set of recordings [one such set is shown in (A)] to 1 and relating the subsequent traces to this value, the current traces were normalized. The data from all sets of recordings were then averaged. In the presence of InsP_6 , the time course of inactivation increased fivefold ($P < 0.01$, Student's t test for paired data). Data were fitted to a single exponential function with the Clampfit program. (C) Typical recording of inward I_{Ca} with the same voltage protocol as in (A), including $10 \mu\text{M}$ InsS_6 in the pipette solution. With increased time, InsP_6 and InsS_6 enter the cytosol through the pipette solution, resulting in an increase in I_{Ca} . (D) Cells were incubated in the absence of InsP_6 or InsS_6 (i) or exposed to InsP_6 , but in the presence of $20 \mu\text{M}$ Cd^{2+} (ii). (E) Compiled data on inward I_{Ca} with InsP_6 in the pipette (●, $n = 30$), in the absence of InsP_6 (▲, $n = 14$), and with the combination of InsP_6 in the pipette and $20 \mu\text{M}$ Cd^{2+} in the bath solution (■, $n = 11$). Data are expressed as integrated current, Q_{Ca} , during the depolarizing step and were normalized by setting the first value in each experiment as the reference point (100%).



two isomers on Ca^{2+} currents. The observation that $\text{Ins}(3,4,5,6)\text{P}_4$ neither inhibited PPase activity nor stimulated Ca^{2+} channel activity supports the concept that inhibition of PPase activity may be part of the mechanism whereby InsP_6 and InsP_5 stimulate Ca^{2+} channel activity. InsP_6 can be readily metabolized by either kinase or phosphatase activity in mammalian cells (25), including insulin-secreting cells (26). However, nonmetabolizable InsS_6 was as efficient as InsP_6 in promoting increased activity of the Ca^{2+} channel (Fig. 3C), and it is therefore unlikely that a metabolite of InsP_6 is responsible for the observed effects.

Because 2 μM InsP_6 had a stimulatory effect on the Ca^{2+} current (24), only a slight suppression of PPase activity may be sufficient to modulate Ca^{2+} channel activity. Alternatively, InsP_6 , in addition to inhibiting PPase activity, may also affect the Ca^{2+} channel by other mechanisms. The

facts that the effect of InsP_6 on Ca^{2+} channel activity is more accentuated than that on PPase activity and that OA is an effective inhibitor of PPase activity but less effective in promoting the Ca^{2+} current indicate that the inositol polyphosphate may have other effects (27, 28). Indeed, InsS_6 had a marked effect on the Ca^{2+} current at a concentration that had only a minor effect on PPase activity.

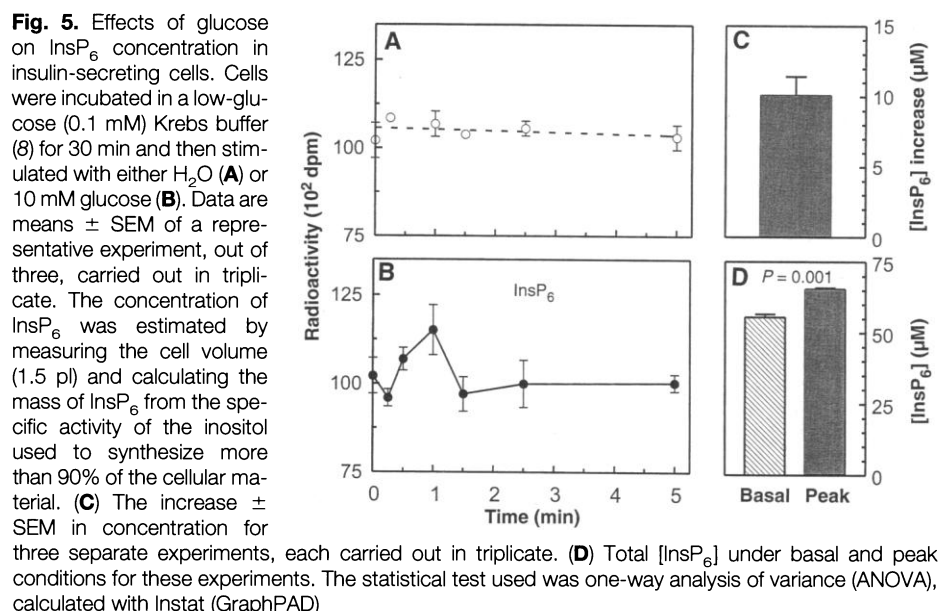
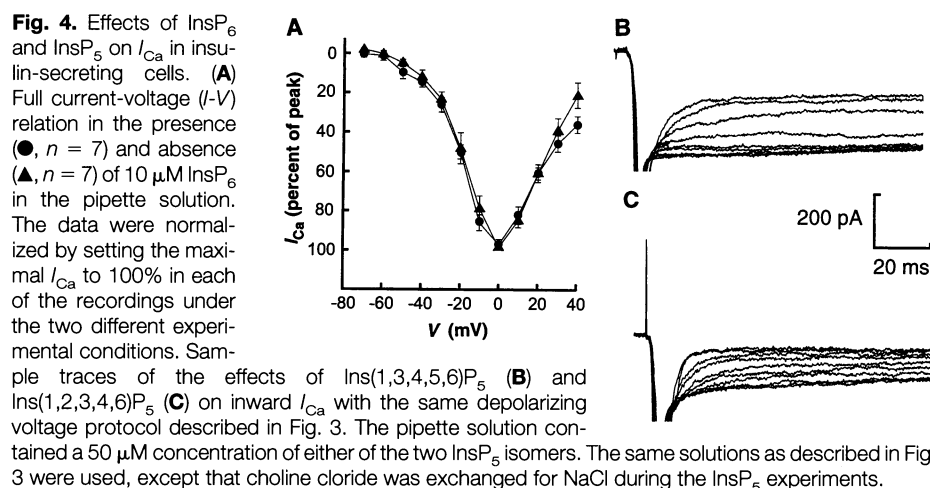
We tested whether intracellular amounts of InsP_6 changed with metabolic and hormonal stimuli. Insulin-secreting cells, which had been incubated with [^3H]myo-inositol, were stimulated with 10 mM glucose (Fig. 5). Under control conditions, there was no change in the concentration of InsP_6 (Fig. 5A). However, there was a consistent increase in the concentration of InsP_6 (10 μM) 1 to 2 min after stimulation of the cells with glucose (Fig. 5, B to D). These results are consistent with a possible modulatory role of this inositol

polyphosphate in β cell signal transduction under physiological conditions.

Increased concentrations of InsP_6 in insulin-secreting cells exposed to glucose, may stimulate activity of voltage-gated L-type Ca^{2+} channels by suppression of serine-threonine PPase activity. Because InsP_6 is localized to membranes (29), it is topographically disposed to regulate ion channels. InsP_6 , which is present in all mammalian cells, may have a fundamental effect in general on protein phosphorylation and cellular regulation.

REFERENCES AND NOTES

1. P. Arkhammar, T. Nilsson, P. Rorsman, P.-O. Berggren, *J. Biol. Chem.* **262**, 5448 (1987).
2. P.-O. Berggren and O. Larsson, *Biochem. Soc. Trans.* **22**, 12 (1994).
3. M. J. Berridge and R. F. Irvine, *Nature* **341**, 197 (1989).
4. S. I. Walaas and P. Greengard, *Pharmacol. Rev.* **43**, 229 (1991); W. A. Catterall, *Annu. Rev. Biochem.* **64**, 493 (1995); O. Krizanova, *Gen. Physiol. Biophys.* **15**, 79 (1996).
5. C. Haby et al., *Biochem. J.* **298**, 341 (1994).
6. C. Åmmälä et al., *Proc. Natl. Acad. Sci. U.S.A.* **91**, 4343 (1994).
7. C. J. Barker and P.-O. Berggren, unpublished data.
8. Clonal HIT cells were plated at 10% of the density required for experiments and allowed to grow for 168 hours in inositol-free medium containing 5.5 mM glucose, [^3H]inositol (2 $\mu\text{Ci}/\text{ml}$) (Amersham International), 50 μM myo-inositol, dialyzed fetal bovine serum (FBS) (10%), penicillin (100 IU/ml), and streptomycin (100 mg/ml). For glucose stimulation experiments, a Krebs buffer containing 109 mM NaCl, 4.6 mM KCl, 1 mM MgSO_4 , 0.15 mM Na_2HPO_4 , 0.4 mM KH_2PO_4 , 35 mM NaHCO_3 , 2 mM Ca^{2+} , 20 mM HEPES (pH 7.4), and bovine serum albumin (BSA) (0.5 mg/ml) was used. Cells were incubated in a low-glucose buffer (0.1 mM) for 30 min and then stimulated with either deionized H_2O (control) or 10 mM glucose. Cell samples were quenched with 5% trichloroacetic acid (TCA) and neutralized by washing with ether, followed by addition of EDTA buffer (pH 7.0) to a final concentration of 10 mM. The samples were stored at -20°C . For separation of multiple inositol phosphate species from the insulin-secreting cells, we performed high-performance liquid chromatography (HPLC) on a 25-cm Whatman Partisphere-SAX column (Laserchrom, Rochester, UK). The column was equilibrated with H_2O , and the sample was loaded and eluted with a gradient generated from deionized H_2O (buffer A) and 1.25 M $(\text{NH}_4)_2\text{HPO}_4$ adjusted to pH 4.4 with H_3PO_4 (buffer B) (0% B from 0 to 5 min, then a linear gradient to 100% B from 5 to 25 min, then 100% B from 25 to 55 min). Samples were collected with a Gilson 202 programmable fraction collector at 0.5-min intervals. Scintillation fluid (Scintillant Ultima Flo AP, Canberra Packard, Groningen, Netherlands) was added to the fractions, and radioactivity was determined by counting with quench correction.
9. P. J. Hughes and R. H. Michell, *Curr. Opin. Neurobiol.* **3**, 383 (1993).
10. Å. Sjöholm, R. E. Honkanen, P.-O. Berggren, *Biosci. Rep.* **13**, 349 (1993).
11. G. Li et al., *J. Biol. Chem.* **267**, 4349 (1991).
12. In Fig. 2, A to D, the catalytic subunits of the protein phosphatases used were purified from rabbit skeletal muscle (PP1) and bovine cardiac tissue (PP2A), as described [P. Cohen et al., *Methods Enzymol.* **159**, 390 (1988)]. The catalytic subunit of PP3 was purified from bovine brain, as described (13). The enzymes were stored at -20°C in 60% (v/v) glycerol-50 mM tris-HCl (pH 7.0), 0.1 mM



EGTA, and 0.1% mercaptoethanol. The proteins were 80 to 95% pure, as estimated by analysis of silver-stained gels. InsP₆ and Ins(1,3,4,5,6)P₆ were from Calbiochem and Sigma. InsS₆ was from Sigma. Ins(1,2,3,4,6)P₆ was synthesized by G. W. Mayr. In Fig. 2E, clonal insulin-producing RINm5F cells were incubated for 5 days in 60-mm culture dishes in RPMI 1640 medium supplemented with FBS (10%). The medium was quickly removed and cells were washed three times in phosphate-buffered saline, scraped off plates in 0.4 ml of 20 mM tris-HCl buffer (pH 7.4) containing 1 mM EDTA and 2 mM dithiothreitol (DTT), and disrupted in a Polytron (Kinematica, Lucerne, Switzerland) homogenizer. Phosphoprotein phosphatase activity was determined as described (75). Assays (80-μl total volume) contained 50 mM tris-HCl (pH 7.4), 0.5 mM DTT, 1 mM EDTA, 30 μg of BSA, 1.6 μM [³²P]phosphohistone, and the appropriate concentrations of inositol polyphosphates or derivatives. After 10 min of incubation at 30°C, 0.1 ml of 14% TCA was added, and the mixture was centrifuged for 5 min at 12,000g. The radioactivity was determined in a 0.1-ml portion of the supernatant.

13. C. Bialojan and A. Takai, *Biochem. J.* **256**, 283 (1988); P. Cohen, C. F. B. Holmes, Y. Tsukitani, *Trends Biochem. Sci.* **15**, 98 (1990); R. E. Honkanen et al., *J. Biol. Chem.* **266**, 6614 (1991).
14. E. Graf, J. R. Mahoney, R. G. Bryant, J. W. Eaton, *J. Biol. Chem.* **259**, 3620 (1987); P. T. Hawkins et al., *Biochem. J.* **294**, 929 (1993); I. D. Spiers et al., *Carbohydr. Res.* **282**, 81 (1996).
15. D. L. Brautigam and C. L. Shriner, *Methods Enzymol.* **159**, 339 (1988).
16. J. Zwiller and P.-O. Berggren, unpublished data.
17. A. B. Theilbert et al., *Proc. Natl. Acad. Sci. U.S.A.* **88**, 3165 (1991).
18. M. Fukada, J. Aruga, M. Niinobe, S. Aimoto, K. Mikoshiba, *J. Biol. Chem.* **269**, 29206 (1994).
19. K. Nogimori et al., *ibid.* **266**, 16499 (1991).
20. J. A. Stuart, K. L. Anderson, P. J. French, C. J. Kirk, R. H. Michell, *Biochem. J.* **303**, 517 (1994); D. Carpenter et al., *Biochem. Soc. Trans.* **17**, 3 (1989).
21. The clonal insulin-secreting cell lines RINm5F and RIN14B were cultured in RPMI 1640 medium for 24 hours, after which the cells were washed with a solution containing 138 mM choline chloride, 5.6 mM KCl, 1.2 mM MgCl₂, 10 mM CaCl₂, 10 mM tetraethylammonium chloride, and 5 mM Hepes (pH 7.4) and then placed in this medium. The pipette solution contained 150 mM *N*-methyl-D-glucamine, 110 mM HCl, 1 mM MgCl₂, 2 mM CaCl₂, 10 mM EGTA, 3 mM Mg-ATP, and 5 mM Hepes (pH 7.15). All experiments were performed at room temperature (22° to 24°C). The whole-cell configuration of the patch-clamp technique [O. P. Hamill, A. Marty, E. Neher, B. Sakmann, F. J. Sigworth, *Pfluegers Arch. Eur. J. Physiol.* **391**, 85 (1981)] was used with an Axopatch 200 patch-clamp amplifier (Axon Instruments). Voltage steps were generated, digitized, and stored with the program pClamp (Axon Instruments) and Labmaster ADC (Scientific Solutions, Solon, OH). The current responses were filtered at 1 kHz with a Bessel filter (-3-dB point).
22. F. M. Ashcroft and P. Rorsman, *Prog. Biophys. Mol. Biol.* **54**, 87 (1989).
23. R. W. Tsien, D. Lipscombe, D. V. Madison, K. R. Bley, A. P. Fox, *Trends Neurosci.* **11**, 431 (1988).
24. O. Larsson and P.-O. Berggren, unpublished data.
25. F. S. Menniti, K. G. Oliver, J. W. J. Putney, S. B. Shears, *Trends Biochem. Sci.* **18**, 53 (1993).
26. C. J. Barker et al., *Biochem. J.* **306**, 557 (1995).
27. A. M. Efanov, S. V. Zaitsev, P.-O. Berggren, *Proc. Natl. Acad. Sci. U.S.A.* **94**, 4435 (1997).
28. R. H. Palmer et al., *J. Biol. Chem.* **270**, 22412 (1995).
29. D. R. Poyner, F. Cooke, M. R. Hanley, D. J. Reynolds, P. T. Hawkins, *ibid.* **268**, 1032 (1993).
30. We thank M. O. Revel for preparation of purified PP1, PP2A, and PP3 and A. Lindgren for technical assistance. Supported by the Swedish Medical Research Council (grants 03x-09890, 04x-09891, and 19x-00034), the Funds of the Karolinska Institute, the Juvenile Diabetes Foundation International, the Nordic Insulin Foundation, the Magnus Bergvalls Foundation, the Swedish Diabetes Association, the Bert

von Kantzows Foundation, the Fredrik and Ingrid Thuring Foundation, and the Association pour la Recherche sur le Cancer (5039) and by grants from the Swedish Medical Research Council, the Swedish

Institute, the Karolinska Institute, and the Swedish Diabetes Association (C.J.B. and J.Z.).

3 June 1997; accepted 4 September 1997

Interneuron Migration from Basal Forebrain to Neocortex: Dependence on *Dlx* Genes

S. A. Anderson, D. D. Eisenstat, L. Shi, J. L. R. Rubenstein*

Although previous analyses indicate that neocortical neurons originate from the cortical proliferative zone, evidence suggests that a subpopulation of neocortical interneurons originates within the subcortical telencephalon. For example, γ -aminobutyric acid (GABA)-expressing cells migrate in vitro from the subcortical telencephalon into the neocortex. The number of GABA-expressing cells in neocortical slices is reduced by separating the neocortex from the subcortical telencephalon. Finally, mice lacking the homeodomain proteins DLX-1 and DLX-2 show no detectable cell migration from the subcortical telencephalon to the neocortex and also have few GABA-expressing cells in the neocortex.

The primary subdivisions of the forebrain, including the neocortex and the basal ganglia, have distinct molecular and cellular properties (1, 2). Previous evidence suggests that these subdivisions develop from separate proliferative zones that do not intermix (3). Here we show that cell migration occurs between the primordia of the basal ganglia and the cerebral cortex. Our results suggest that many neocortical interneurons are generated by the proliferative zone of the basal ganglia.

Neocortical neurons include two types: the excitatory pyramidal neurons and the inhibitory (GABA-containing) interneurons. During development, neocortical neurons were thought to derive from the proliferative zone of the neocortical primordium. However, studies of neuronal migration in vitro indicate that cells migrate from the lateral ganglionic eminence (LGE) (4), which is the primordium of the striatum (5), into the neocortex. Other evidence suggests that these cells might be interneurons. For example, clonally related GABA-containing cells tend to be more dispersed across the neocortex than are clones of pyramidal neurons (6); there are GABA-containing cells in the intermediate zone (IZ) at the transition between the LGE and the neocortex, which have a morphology of tangentially migrating cells (7); and interneurons migrate tangentially from the subventricular zone

(SVZ) near the cortical-striatal junction into the olfactory bulb (8).

To investigate the migration of subcortically derived cells into the neocortex, we used a slice culture preparation (9). Crystals of 1,1'-dihexadecyl-3,3,3'-tetramethylindocarbocyanine perchlorate (DiI) were placed into the LGE of embryonic day 12.5 (E12.5) mice; after 36 hours in culture, many labeled cells were detected in the neocortex (Fig. 1A). This migration begins on about E12.5, as only a few labeled cells reached the cortex from E11.5 slices that were grown in culture for 36 hours (10). Many of the DiI-containing cells in the neocortex look like tangentially migrating cells, with leading processes tipped by growth cones and a trailing process (Fig. 1, A and F).

Calbindin is present in cells resembling the tangentially oriented GABA-containing cells that are found in the IZ of the developing neocortex (7, 11). To determine whether cells migrating from the LGE into the neocortex express calbindin or GABA, DiI was inserted into the LGE of slices from E12.5 to E14.5 mice; the slices were then incubated for 30 hours and resectioned. GABA (Fig. 1, B through E) or calbindin (Fig. 1, G through J) immunofluorescence was present in about 20% of DiI-labeled neocortical cells (12).

To provide additional evidence for the migration of GABA- and calbindin-expressing cells from the subcortical telencephalon to the neocortex, we made slice cultures that were transected at the cortical/subcortical angle on one side. After 40 hours in vitro, the neocortical IZ on the transected sides had about 10 times fewer GABA- (13, 14) and calbindin-expressing cells (Fig. 2, A through C) than on the

Nina Ireland Laboratory of Developmental Neurobiology, Center for Neurobiology and Psychiatry, Department of Psychiatry and Programs in Neuroscience, Developmental Biology, and Biomedical Sciences, 401 Parnassus Avenue, University of California at San Francisco, CA 94143-0984, USA.

*To whom correspondence should be addressed. E-mail: jllr@cgl.ucsf.edu